Voorhoeve, R. J. H., "Organohalosilanes, precursors to silicones," Elsevier Publishing Co. (1967).
Wakao, N., and J. M. Smith, Diffusion in catalyst pellets," *Chem. Eng. Sci.*, **17**, 825 (1962).
Wen, C. Y., and S. C. Wang, "Thermal and diffusional effects in noncatalytic solid gas reactions," *Ind. Eng. Chem.*, **62**(8), 30 (1970).
Wen, C. Y., and L. Y. Wei, "Simultaneous non-isothermal non-catalytic solid-gas reactions," *AIChE J.*, **17**, 272 (1971).
Wen, C. Y., and N. T. Wu, "An analysis of slow reaction in a porous particle," *AIChE J.*, **22**, 1012 (1976).
Wen, C. Y., "Non-catalytic heterogeneous solid-fluid reaction models," *Ind. Eng. Chem.*, **60**, 34 (1968).
Wouterlood, H. J., "The reduction of ilmenite with carbon," *J. Chem. Tech. Biotechnol.*, **29**, 603 (1979).
Yagi, J. and J. Szekely, "Effects of gas and solids maldistribution on the performance of moving bed reactors, reduction of iron oxide pellets with hydrogen, *AIChE J.*, **25**, 800 (1979).

Manuscript received October 29, 1981; revision received June 16, and accepted June 29, 1982.

Shear History Effects in the Spinning of Polymers

During their industrial processing, polymer liquids are usually subjected to complex flow histories. In principle, these can be taken into account in the constitutive equations. In reality, difficulties arise for complex flows. This fact can be illustrated by the spinning process. Here, experiments are presented in which the upstream section of a spinning device has been changed systematically. A constitutive model and a calculation procedure are suggested that permit an analysis of the upstream effects in the spinning flow. The results indicate that this analysis predicts well the spinning dynamics in the present experiments, using shear flow characteristics for the liquids. It is also concluded that the spinning flow can be altered by upstream changes. The changes in structure seem to be the most pronounced ones.

JAN MEWIS and GUIDO De CLEYN

**Department of Chemical Engineering
Katholieke Universiteit Leuven
B-3030 Leuven, Belgium**

SCOPE

The fluid mechanics of polymer processing constitutes an industrial problem that has not been completely solved. Elongational flows, in particular transient ones as in spinning, turn out to be difficult to describe (Denn, 1980). Attempts to model spinning dynamics with rheological characteristics derived from shear flow data, have show systematic errors (Spearot and Metzner, 1972; Bankar et al., 1977; Chang and Denn, 1979). Some promising results using relaxation time distributions should, however, be mentioned (Phan-Thien, 1978).

An additional problem arises in the case of spinning. This type of flow is always preceeded by an upstream flow in a tube and a nozzle. The resulting initial conditions for the spinning line are normally incorporated in a rather arbitrary manner. Experimentally some shear history effects have been found by Oliver and Ashton (1976), but no quantitative interpretation was given.

Considering the more general interest of shear history effects in complex processing flows, some systematic experiments were performed. They include spinning flow with a variable shear history. As rheological constitutive equation, a structural kinetics model is used (De Cleyn and Mewis 1981) derived from that by Acierno et al. (1976). Model predictions of the spinning dynamics are used to assess the rheological model and to investigate the effect of shear history.

CONCLUSIONS AND SIGNIFICANCE

The suggested rheological model makes it possible to take into account relatively complex shear histories in spinning experiments. If the shear rate is not constant throughout the cross section, as in pipe flow, averaging over the structure distribution gives better results than averaging over the shear rate. The stress levels at the nozzle can be estimated directly as long as they are not affected by the spinning column. Experimentally some effect of flow history on the spinning dynamics of the polymer solutions under investigation is detected. However, the global effect is reduced somewhat by a compensation in the spinning flow. The interference becomes more obvious if the resulting structures are calculated. The effect can be associated with structural changes of a suitable characteristic time scale.

The rheological model and the calculation procedure used here provide a means to analyze relatively complicated flow patterns and suggest a route to the rational analysis of polymer processing operations. The model can also be used in numerical simulations. Further elaboration will be necessary in order to handle the even more complex situations of industrial processes.

Present address of G. De Cleyn: Essochem N. V., Zwijndrecht, Belgium.

Polymers liquids, either solutions or melts, belong to the class of viscoelastic materials. Hence they have a finite and fading memory for their mechanical history. This specific aspect of the rheological behavior can be verified easily by doing transient measurements. Available constitutive equations describe qualitatively the phenomena under consideration. Quantitatively, the desired accuracy is not always achieved, especially in transient behavior. Spinning (Agrawal et al., 1977) and intermittent shear flow (Lodge, 1964) can be mentioned in this respect.

In industrial processes, the flow patterns are often complex. Combined with the difficult rheological nature of the polymer, it explains why very few processing techniques can be analyzed accurately (Middleman, 1977). Even the presently available numerical techniques have not provided a satisfactory solution. It could be considered that some progress could be made by studying flows of intermediate complexity between that of industrial processes and that of normal laboratory devices. This is the approach followed here to verify whether changes in shear history could be used to control the material behavior in a technical process. Oliver and Ashton (1976) presented experiments of this nature and found differences which they attribute to shear history effects. Somewhat surprisingly, the effects were most pronounced with only slightly viscoelastic fluids. In addition, no attempt was made to correlate the measured effects with material parameters or with a constitutive equation. Hence, there is no basis available for a systematic discussion or application of the discussed phenomena in polymer processing.

Solution of the previous problem requires a suitable spinning device in which various shear histories can be applied in the upstream section. In addition a suitable rheological constitutive equation and a corresponding calculation procedure should be selected. The rheological model should keep track of shear effects and this in such a manner that dynamic calculations can be made for the flows under consideration. Structural kinetics models (Mewis, 1979) are particularly suitable in this respect. They follow the instantaneous structure under shear by means of a structural parameter. Hence, it becomes easy to compare the effects of various shear histories. Still it remains to be verified whether these models describe accurately polymer behaviour under the relatively complicated test conditions which are of interest here.

EXPERIMENTAL

In order to create a variable but tractable kinematic history, the sample is initially pumped through a long tube (Figure 1).

In this manner accidental effects of earlier history are eliminated, at the same time the material is brought in a known equilibrium condition. The liquid is fed to the tube from a cylindrical reservoir (1.15 l). A second reservoir is available either as an extra volume of material or for deaeration purposes. A constant flow rate is realized by means of a piston which is driven from an Instron 3211 capillary rheometer. In the present experiments flow rates between 3.60×10^{-8} and 1.20×10^{-6} m^3/s have been used. The initial tubular section has a length of 50 cm and an inner diameter of 9 mm. It is followed by an interchangeable section 8 cm long. The following sections have been used:

a) Empty tube, inner diameter of 9 mm, serves as a reference condition.

b) Tube with a lateral rod, diameter 3.0 mm, 22 or 58 mm from the entrance of the section.

c) A cylindrical insert of diameter 6.5 mm to produce annular flow.

d) Geometry as sub *c* but with rotation of the inner cylinder at 12.5 rpm to produce torsional flow.

e) Porous bed by filling the tube with 175 glass spheres, diameter 3.0 mm and hydraulic radius of the bed 0.59 mm, bed porosity is 0.37.

f) Insertion of 14 parallel capillaries, each with a diameter of 1,45 mm.

The various inserts can be characterized by means of rough estimates for average shear rate and average residence time for a flow rate of 0.36×10^{-6} m^3/s:

Insert	Avg. Shear Rate (s^{-1})	Avg. Residence Time(s)
a	2.5	Equilibrium Reached
b	7	12
c	30	7
d	30	7
e	—	5
f	40	5

The interchangeable section is followed by a conical nozzle with a length of 5 mm and a cone angle of 24°. The liquid jet that leaves the nozzle is taken up and stretched by a rotating wheel located 15 cm below the nozzle. By changing the flow rate and the takeup speed, the total stretching of the spinning line can be varied between 2 and 50. The spinning line is much thicker than in industrial processes, but this does not affect the parameters that are relevant for our purpose.

The kinematics of the jet are derived from its geometry as measured from a photographic picture. In order to measure the force F_N exerted by the jet on the nozzle, part of the tubular section has a wall thickness of 0.25 mm. It serves as a torsion bar and eliminates the need for a flexible coupling. The displacement of the nozzle under tension is detected with a linear displacement transducer. The force measuring range of the device covers 10^{-5} to 10^{-1} N. It has been verified that static pressures up to 13 bar do not affect the force reading. The transducer meter is calibrated by adding weights to the nozzle.

The local internal stress in the spinning line is calculated from F_N through a momentum balance.

$$\sigma_{zz} - \sigma_{rr} = \frac{1}{\pi R^2}\left(F_I + F_N + F_F - F_G - \frac{1}{2}F_S\right) \tag{1}$$

The air friction is calculated from:

$$F_F = 2\pi \int_o^z R\, F_D\, dz$$

with (Ziabicki, 1976)

$$F_D = 0.843\, \rho_a v^2 \left(\frac{\eta_a z}{\rho_a R^2 v}\right)^{0.915}$$

where

$$F_S = 2\pi R \sigma_s$$

In the present experiments some forces are systematically much smaller than F_N:

$$F_I/F_N < 0.1\%$$

$$F_F/F_N < 0.001\%$$

$$F_S/F_N < 10\%$$

The local stretching rate $\dot{\epsilon}$ is defined as:

$$\dot{\epsilon} = \frac{dv}{dz} \tag{2}$$

assumed constant throughout the cross section of the liquid column. It is computed from the flow rate Q and the value of the local jet diameter D through a mass balance:

$$\dot{\epsilon} = \frac{8Q}{\pi D^3}\frac{dD}{dz} \tag{3}$$

In order to avoid an amplification of errors in the required differentiation

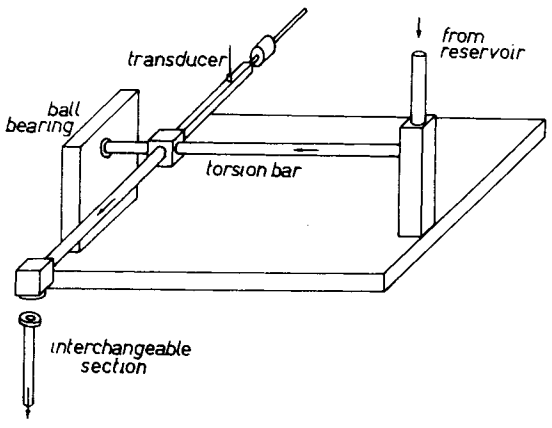

Figure 1. Schematic diagram of the spinning apparatus.

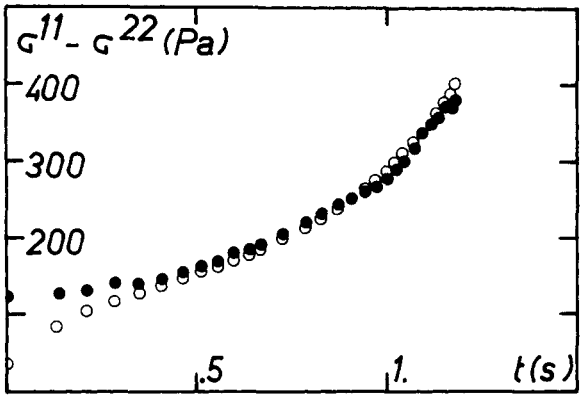

Figure 2. Testing the accuracy of the spinning device, comparison between stress values calculated from the momentum balance and these calculated using the shear viscosity (○: from shear viscosity, ●: from spinning experiment) (liquid: PIB, η = 28.3 Pa·s).

of the measured profile $D(z)$, the latter is smoothed by applying curve fitting. The Kanel method (1972), basically a power law approximation, has been shown to be successful in a number of cases but fails to describe maxima or minima in the $\dot{\epsilon}$-curve. Instead, a five-parameter model is used here:

$$D = a_1(z + a_2)^{-a_3} \exp\left(\frac{a_4}{z + a_5}\right) \tag{4}$$

It reduces to the power law kinematics when $a_4 = 0$. The main advantage of Eq. 4 is that it can be applied from the nozzle on rather than from an arbitrary distance below the nozzle. Combining Eqs. 3 and 4 one obtains the working equation for the stretching rate:

$$\dot{\epsilon} = \frac{8Q}{\pi D^2}\left[\frac{a_4}{(z + a_5)^2} - \frac{a_3}{(z + a_2)}\right] \tag{5}$$

The time elapsed since leaving the nozzle is given by:

$$t = \frac{\pi}{4Q}\int_o^z D^2 dz \tag{6}$$

The values of the parameters in Eqs. 4 and 5 are determined from 22 data points by means of a nonlinear parameter estimation technique. From the 50 runs performed 44 could be described with a correlation coefficient of at least 0.999. The remaining tests showed a poorer quality of the picture, the lowest correlation coefficient was 0.9945. The performance of the spinning device has been evaluated by running a Newtonian liquid. A low MW polyisobutylene oil (Oppanol B3 from BASF, η = 28.3 Pa·s) is used for this purpose (Figure 2).

The correspondence between calculated and measured stress levels is good. The initial discrepancy extends roughly one diameter from the nozzle. In this region, the velocity profile is not flat (Fisher et al., 1980). Consequently, the purely elongational flow is not developed yet and the analysis based on Eq. 2 does not apply.

Two polymer solutions are used in the experiments. The first is a solution of polyisobutylene (MW 380.000, Oppanol B50 from BASF) in decaline at a concentration of 250 g/L. The second contains polyacrylamide (Separan AP 30 from Dow) in a 50/50 mixture of water and glycerine at a concentration of 15 g/L. At the shear rates that occur in the present experiments the two fluids have a power law index of 0.33. Both samples have been studied in detail under shear flow (De Cleyn and Mewis, 1981).

THEORETICAL

From a theoretical point of view, two requirements have to be met. First, a suitable constitutive model must be selected. It should be sufficiently accurate yet still tractable under the kinematic conditions of interest. Possibly it should reflect in a direct manner the effect of shear history. The second theoretical requirement refers to the analysis of the variable shear history itself.

Shear effects can be accounted for in a constitutive equation by introducing a variable structural parameter. This parameter expresses the instantaneous degree of structure. Its rate of change is associated with the flow conditions in a separate kinetic equation. This structural kinetics approach has been applied on various groups of materials; a recent review is available (Mewis, 1979). The

TABLE 1. LINEAR SPECTRA FOR THE TWO LIQUIDS

$\tau_{i,o}$ (s)	Oppanol B50 $G_{i,o}$ (Pa)	Separan AP30 $G_{i,o}$ (Pa)
0.0001	240	—
0.000316	184	240
0.001	132	180
0.00316	110	100
0.01	83.5	45.0
0.0316	63	26.3
0.1	49	21.9
0.316	34	18.2
1	21	15.2
3.16	15	12.7
10	6	10.5
31.6	—	8.7
100	—	7.3
316	—	6.0
1000	—	1.0
3160	—	0.1
10000	—	0.01

model which will be used here is derived from that of Acierno et al. (1976). It is based on a generalized convective Maxwell model. The Maxwell parameters are made history dependent through the structural parameter x_i:

$$\underline{\underline{\sigma}} = \sum_{i=1}^{n} \underline{\underline{\sigma}}_i \tag{7}$$

$$\frac{\underline{\underline{\sigma}}_i}{G_i} + \tau_i \frac{\delta}{\delta t}\left(\frac{\underline{\underline{\sigma}}_i}{G_i}\right) = 2\tau_i \underline{\underline{D}} \tag{8}$$

$$\frac{\delta}{\delta t}\left(\frac{\underline{\underline{\sigma}}_i}{G_i}\right) = \frac{d}{dt}\left(\frac{\underline{\underline{\sigma}}_i}{G_i}\right) - \underline{\underline{\nabla v}} \cdot \left(\frac{\underline{\underline{\sigma}}_i}{G_i}\right) - \frac{\underline{\underline{\sigma}}_i}{G_i} \cdot \underline{\underline{\nabla v}}^T \tag{9}$$

$$G_i = G_{i,o} x_i \tag{10}$$

$$\tau_i = \tau_{i,o} x_i^{1.4} \tag{11}$$

$$\frac{dx_i}{dt} = \frac{A}{\tau_i^{0.3}}\left(\frac{1}{1 + a\sqrt{\frac{I\sigma_i}{2G_i}}} - x_i\right) \tag{12}$$

The present model differs from Acierno's by the kinetic equation (Eq. 12). The need for this difference has been demonstrated elsewhere (De Cleyn and Mewis, 1981) where also the characteristics of the two solutions have been determined from shear flow data. The linear zero shear-spectra are represented in Table 1.

From the viscosity curves, the constants a of Eq. 12 have been calculated:

$$a = 1.0 \text{ (PIB)}$$

$$a = 0.85 \text{ (PAA)}$$

For the PIB solution the constant A of Eq. 12 has been derived from transient shear flow data:

$$A = 0.2 \text{ (PIB)}$$

On the other hand, this parameter will be derived from transient elongational flow data for PAA.

With the set of Eqs. 7–12, one still needs a procedure to compute the effect of the flow history on structure. Following each individual liquid element throughout a complex process is not very practical. Therefore, the possibility to apply averaging techniques was considered. The nonlinear relation of Eq. 12 between structure and flow does make the use of an average shear rate in a cross section rather unsuitable (De Cleyn, 1980). Instead, advantage is taken of the specific nature of the constitutive model and the averaging is performed on the structural parameters x_i. A volume average is taken which can be understood to represent a mixing of the resulting structures.

Under equilibrium tube flow and related geometries, the aver-

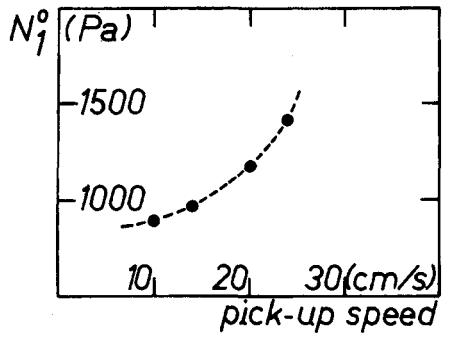

Figure 3. Effect of pick-up speed of the spinning line on the average stress at the nozzle exit (PAA, flow rate = 0.36 × 10^{-6} m^3/s).

ages $\bar{x}_i$ are then calculated from the velocity distributions through:

$$\bar{x}_i = \frac{\int_o^R 2\pi r v_z(r) x_i(r) dr}{\int_o^R 2\pi r v_z(r) dr} \tag{13}$$

The resulting set of values $\bar{x}_i$ does not correspond to any one calculated at equilibrium from Eqs. 7–12. It can be seen that the latter lead to:

$$\frac{1 - x_i}{x_i^{2,4}} = a\tau_{i,o}\dot{\gamma} \tag{14}$$

Equation 14 can be used to allocate an average shear rate $\bar{\dot{\gamma}}_i$ to each individual value $\bar{x}_i$. In this manner, the average stress in a cross section can be calculated for each Maxwell element. Under transient flow conditions the average stress is derived from the contributions of the individual Maxwell elements for the imposed $\bar{\dot{\gamma}}_i$ and the average residence time.

The afore-said procedure still fails in the nozzle where shear flow and elongational flow occur simultaneously. In addition, there might be an upstream effect from the spinning line especially at high spinning rates (Figure 3). At low spinning rates this effect can be neglected. Based upon the profiles of Cable and Boger (1976), one finds for small cone angles φ that the ratio $\dot{\epsilon}/\dot{\gamma}$ is a constant with a linear average:

$$\frac{\dot{\epsilon}}{\dot{\gamma}} = c_l = \frac{(n + 1)(2n + 1)}{n(3n + 1)}\varphi \tag{15}$$

and a volumetric average:

$$\frac{\dot{\epsilon}}{\dot{\gamma}} = c_v = \frac{(3n + 2)}{(3n + 1)}\varphi \tag{16}$$

The factors c_l and c_v depend on cone angle and power law index.

All experiments have been performed with a single cone. Further, the two liquids used here have identical power law indices. Hence, c remains constant throughout all the tests. Calculated values for c_l and c_v are respectively 0.704 and 0.315. In further work, an empirical value is used, derived from a single run on PAA with a flow rate of 0.360 cm^3/s. One finds:

$$c_{exp} = 0.593 \tag{17}$$

This value is obtained by adapting the calculated stress at the nozzle exit to the measured value.

The kinematics in the nozzle entrance, $\bar{\dot{\gamma}}_i(o)$, are derived from the average shear rates in the preceding tube flow section. With the purely geometrical factor B, the $\bar{\dot{\gamma}}_i$ are approximated by:

$$\bar{\dot{\gamma}}_i(z) \cong \frac{B^3}{(B - z)^3}\bar{\dot{\gamma}}_i(o) \tag{18}$$

The extension rates now follow from Eq. 17 and 18. This procedure was applied on four other runs including one on a polyisobutylene solution. In each case the empirical constant of Eq. 17 was used, Table 2. The correspondence with the measured stresses is considered adequate. Larger cone angles cannot be analyzed in this manner (Cogswell, 1978; Petrie, 1979).

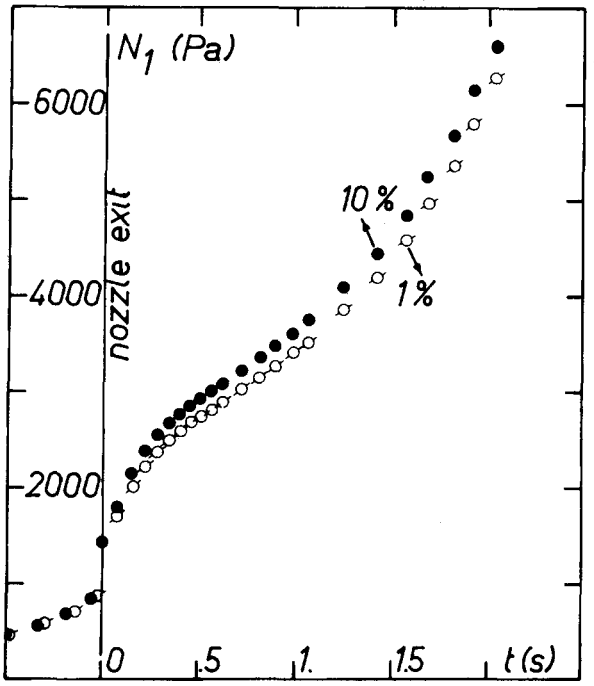

Figure 4. Effect of the assumed penetration depth of spinning line interference within the nozzle.

The whole previous discussion is based on the assumption that the liquid column which leaves the nozzle does not exert any influence in the upstream direction. This condition is only satisfied in the limiting case of low spinning rates (Figure 3). Obviously, it is of interest to calculate other than the limiting low stretching flows. Unfortunately, no suitable calculation procedure seems to be available. Therefore, one recurs to an empirical approximation. From Figure 3, it can be seen that the stresses at the die exit can grow rather rapidly with increasing spinning ratios. It is likely then that, to a first approximation, the increased elongational rates in the nozzle are responsible for the high stresses. Extension has a much greater effect on the diagonal stresses than simple shear.

For these reasons the spinning line effect is dealt with by an increase in c_{exp} (Eq. 17). One would expect the effect only to penetrate upstream to a limited extent (Denn, 1980), but a quantitative technique to estimate the penetration in the nozzle is still lacking. Fortunately the final results are not very sensitive to the detailed value of the penetration depth.

As an illustration stresses in the spinning line have been calculated with two different assumptions (Figure 4). In this particular experimental case, the stress at the exit is more than 50% above the limiting low extension value: 1,420 Pa vs. 890 Pa. The increase can be described by letting c change linearly from 0.593 (Eq. 17) to 2.45 over the last 10% of the nozzle length. Alternatively, a linear increase from 0.593 up to 18.3 in the last 1% of the length gives an identical stress value. The two flow patterns result in identical stresses at the die exit but not in identical structures of the liquid. However, only the shortest relaxation times show marked differ-

TABLE 2. VERIFICATION OF THE NOZZLE CONSTANT BY MEANS OF EXIT STRESSES

Material	Flow Rate (m^3/s) 10^6	Exit Stress (Pa) Exptl.	Calcul.
PAA	0.0360	278	305
PAA	0.120	523	589
PAA	1.201	1590	1590
PIB	1.201	550	552

ences. The latter do not contribute significantly to the spinning stresses (Figure 4).

It should be pointed out that by fitting the stress at the die exit, the initial structure of the spinning zone is completely determined. Any error in modeling the structure resulting from the upstream flow could still give the right value for the initial stress. However the spinning dynamics would be described with an erroneous structure. The possible extent of this error will be discussed below.

The spinning zone itself is analyzed in a similar manner as the shear flow zone and the nozzle. The stresses are now assumed to be constant in any cross section, no averaging is necessary except in the initial part. Swelling occurs at the die exit if the spinning rate is small. A complex flow pattern then arises owing to relaxation and the corresponding cross flow. Some balancing between the two phenomena is assumed whereby structural growth is roughly compensated by structural breakdown. The data with limiting low stretching rates seem to support this approximation. A final test will be provided by the comparison between measured and calculated stresses in the subsequent spinning experiments. In order to reach a sufficient level of accuracy, isothermal tests are required. In nonisothermal spinning, the stress profiles are affected by thermal and history effects and by the interactions between both.

SPINNING FLOW

The proposed model description of Eqs. 7-12, together with the calculation procedure described above, have been used to analyze

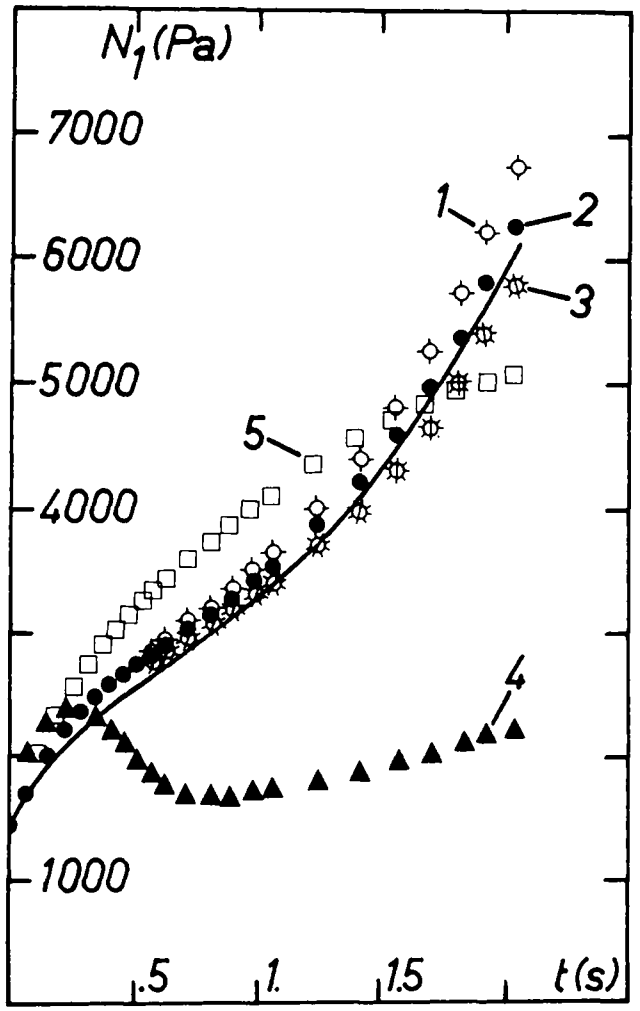

Figure 5. Sensitivity of spinning results to model parameters (1: calculated with $A = 1.1$; 2: with $A = 1.2$; 3: with $A = 1.3$; 4: calculated from the model of Acierno et al.; 5: calculated with $A = 1.2$ but with a shear history incuding additional torsional flow).

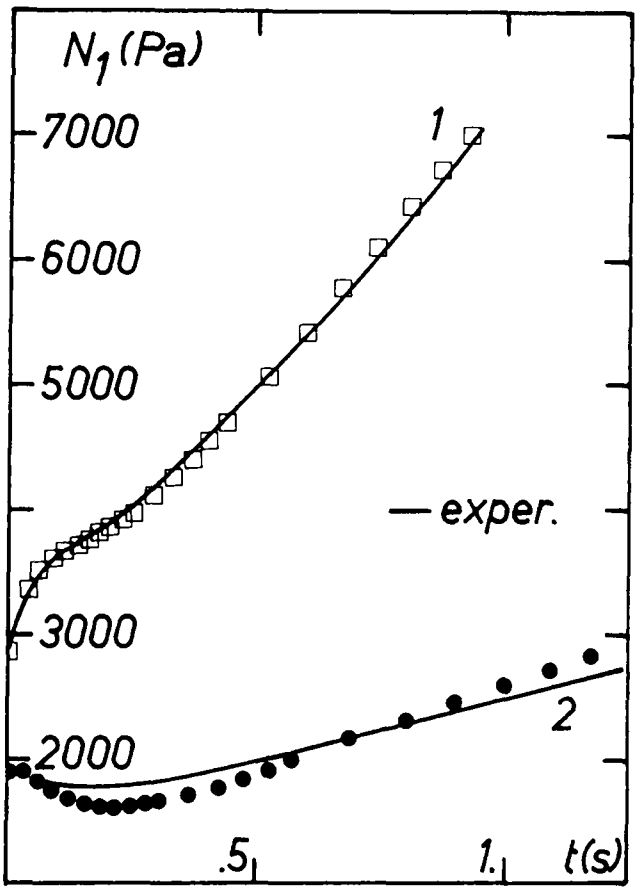

Figure 6. Prediction of stress levels in spinning for PAA; flow rate = 1.20×10^{-6} m³/s (curve 1: pick-up speed = 0.485 m/s; 2: pickup speed = 0.242 m/s).

stress levels in spinning experiments. For the PIB solution, the material parameters obtained from simple shear flow data will be used. For the PAA solution, all but one parameters are derived from simple shear flow. The kinetic parameter A will be derived from a transient elongational flow experiment, i.e. a spinning test (Figure 5). In this test, the shear history is tube flow without any inserts. The stress profile is well predicted with $A = 1.2$ (PAA).

This value also describes well transients in shear flow as published elsewhere (De Cleyn and Mewis, 1981). It clearly differs from the value found for the PIB solution: $A = 0.2$, which indicates the need for an additional parameter in the original Acierno model. As

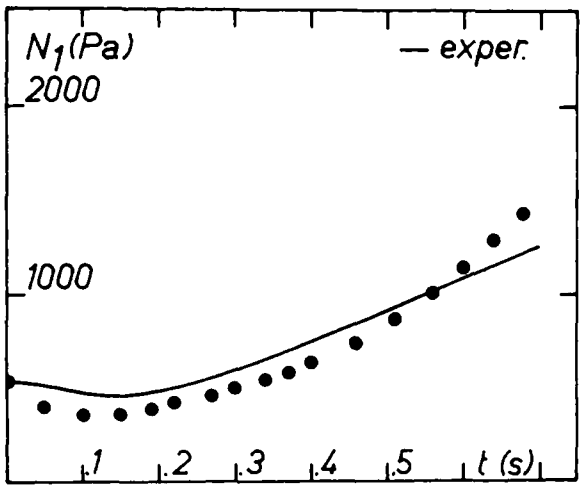

Figure 7. Prediction of stress levels in spinning PIB (flow rate = 1.20×10^{-6} m³/s; pickup speed = 0.337 m/s).

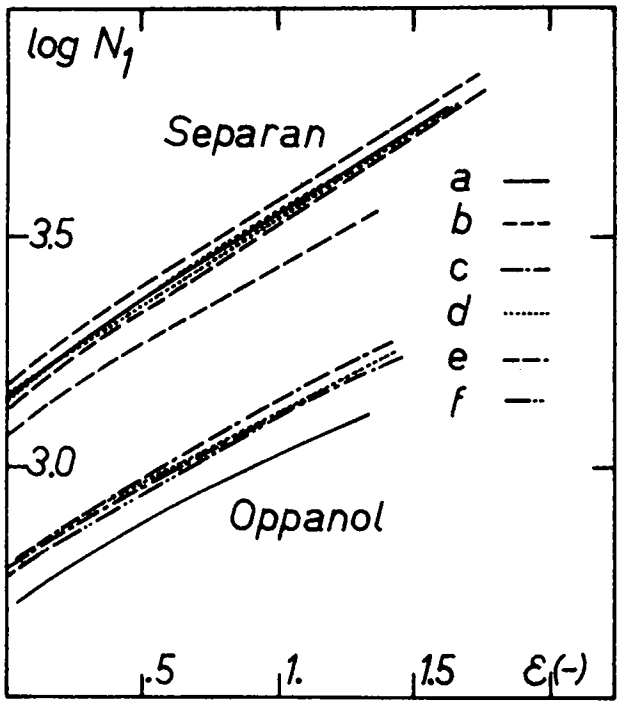

Figure 8. Stress-total strain curves for experiments that differ only in shear history—pickup speed = 0,337 m/s (curves 1: PAA – flow rate = 0.36×10^{-6} m^3/s; curves 2: PIB – flow rate = 1.20×10^{-6} m^3/s).

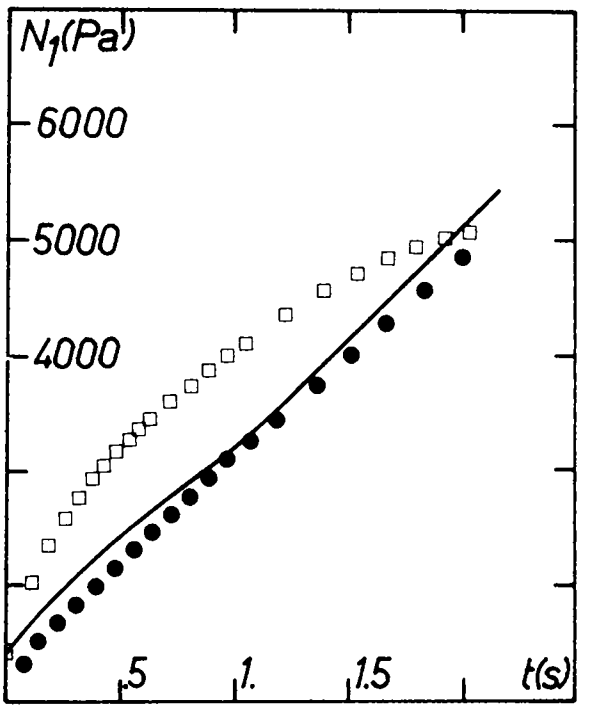

Figure 9. Effect of the shear history on predicted stress levels, PAA, flow rate = 0.36×10^{-6} m^3/s, pickup speed = 0.337 m/s (●: with correct history, □: neglecting the torsional flow).

further proof for this conclusion, the prediction with the Acierno model is also reproduced in Figure 5. The said model results in a structure at the die exit that is broken down too far, especially at the largest relaxation times. Consequently it fails to describe the upturn in stress. Figure 5 also shows the result of using a different initial structure to predict the stress levels. The shear history used is calculated from an experiment in which torsional flow was superimposed on the tube flow (insert *d*). The obvious difference with the experimental values proves the sensitivity of the analysis and the effect of shear history on spinning flow.

The experimental value for *A* can be used to describe spinning experiments with the same material at other flow rates and spinning ratios (Figure 6). A more severe test can be made with the PIB solution. The material parameters are already completely determined as well as the nozzle constant. For low stretching tests no single adaptable parameter is left. For high spinning ratios the same procedure as for PAA is used (Figure 7).

It is concluded from Figures 6 and 7 that the model description presented here describes adequately spinning experiments. This is a severe test for any rheological model and especially if shear flow characteristics are used (Denn, 1977). No other experiment was found in the literature where the stress levels had been computed for a viscoelastic fluid without using any measured parameter.

Up to now only tube flow preceded the nozzle. In a following step the interchangeable sections have been introduced and again the spinning behavior has been analyzed. First, the effect of the shear history on the stress-strain curves is considered (Figure 8). The curves for the various histories nearly coincide. If stress is plotted against time a slightly different picture emerges. The latter curves are somewhat more sensitive to the spinning conditions. A small shear history effect shows up now. At the long times, i.e., 2 seconds, the systems causing high shear rates (systems *c*, *d*, *e*, *f*) show less increase in stress than the weak flows, exemplified by simple tube flow. At the same time, the strain rate-time curves tend to decrease continuously instead of rising near the end of the spinning column.

On the whole, the dynamics and kinematics of spinning do not show a spectacular effect of shear history here. The other process parameters dominate by far. Oliver and Ashton (1976) found more pronounced upstream effects. Different materials are used here as well as different conditions. Lacking a full characterization of Oliver's samples, a comparison is impossible. If the values for the product of average relaxation time with extension rate are compared, they are found to be about five times higher in the present experiments than in Oliver's. One would then expect the detection of history effects to be easier here. The suitability of the way Oliver presents his data can be questioned (Petrie, 1979).

In order to assess in more detail possible differences owing to flow history the corresponding structural changes are considered. As an example, a torsional flow history is selected; interchangeable element *d* (Figure 9).

The model and the calculation procedures outlined above provide a good prediction of the stress levels. If tube flow history is assumed instead of torsional flow, the same spinning kinematics results in a poor prediction of the stress levels. This result confirms the conclusion from Figure 5 about the influence of upstream effects. Indeed the torsional flow is found to break down relaxation mechanisms in a limited range of relaxation times (Figure 10). Here this range roughly extends from 10^{-1} to 10^3 s. During the initial part of spinning the more complete structure produces higher

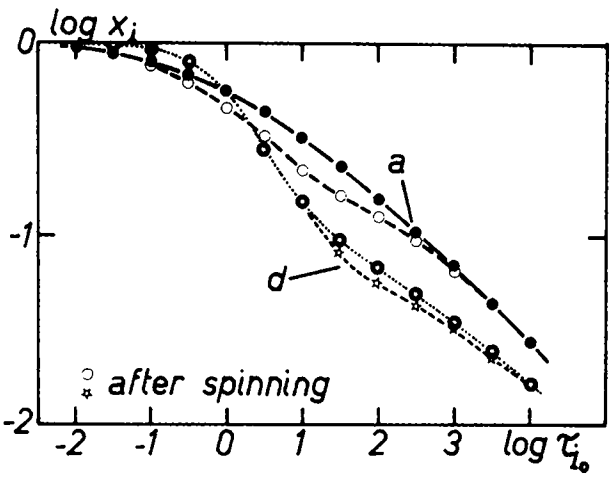

Figure 10. Changes in structural parameters owing to shear history and under spinning (conditions of Figure 9).

stresses although the difference grows smaller with time (Figure 10).

From the kinetic Eq. 12, it follows that structural breakdown is always delayed in time with respect to stress. Consequently, higher initial structures will always cause higher stress transients. In spinning experiments, the global spinning ratio is kept constant. Hence, a weaker structure will still be stretched to the same extent as a less disturbed one. The material can only adapt the strain rate curve, which in this particular case will be smoothed out. In the beginning, the strain rates will be higher than in the more structurized sample. Near the end, the difference will be in the opposite direction. In this manner, the expected stress differences are strongly reduced. The material compensates the differences in its history in much the same way as it is able to compensate perturbations in the spinning flow. This behavior explains the limited differences encountered in the stress and strain rate curves. The way in which the spinning data can be fitted seems very promising and compares favorably with results in the literature. Apparently only the work of Phan-Thien (1978) gives comparable results. The latter requires a parameter for stress saturation which cannot be predicted from shear data. Both models use a distribution of relaxation times. The present results, Figures 5–10, seem to indicate that this information about the spectrum is essential. Model calculations by Denn (1979) lead to the same conclusion.

CONCLUSIONS

Spinning data are presented with two polymer solutions, the rheological properties of which are known rather in detail. In some experiments the upstream shear history has been modified. A rheological model is used which describes the liquids by means of their linear relaxation spectrum and two additional parameters. These two parameters can be obtained from experiments in shear flow.

Application of the model to the spinning dynamics gives a good correlation with experimental data. As this is a structural kinetics model it can describe differences in shear history. It is shown that these differences give rise to relevant changes in predicted stress profiles. Only incorporation of the correct history results in good stress predictions. For one sample spinning stresses under low stretching rates are calculated without using the nozzle exit stresses.

Both the quality of fitting the data and the detailed information between structure and behavior which are presented here suggest potential applications in the analysis of polymer processing.

ACKNOWLEDGMENT

G. De Cleyn received a I.W.O.N.I. fellowship during part of this project. J. Mewis acknowledges hospitality from the University of Delaware during the preparation of the final manuscript. The opportunity to discuss this work with A. B. Metzner and M. M. Denn is greatly appreciated.

NOTATION

A = model parameter, Eq. 12 ($s^{0.30}$)
a = model parameter, Eq. 12 (dimensionless)
a_i = curve fitting parameter for the jet shape, Eq. 4
B = geometrical factor, Eq. 18 (m)
c_1, c_v = linear and volumetric averages of the ratio $\dot{\epsilon}/\dot{\gamma}$ in converging flow (dimensionless)
c_{exp} = experimental value for the ratio $\dot{\epsilon}/\dot{\gamma}$ (dimensionless)
$D(z)$ = local jet diameter (m)
F_D = stress caused by air drag (Pa)
F_F = friction force caused by air drag (N)
F_G = gravity term in the momentum balance of the jet, Eq. 1 (N)
F_I = inertia term in the momentum balance of the jet, Eq. 1 (N)
F_N = measured force exerted on the nozzle by the jet (N)
G_i = shear modulus of Maxwell element i (Pa)
I = first invariant (Pa)
n = power law index (dimensionless)
Q = volumetric flow rate (m^3/s)
$R(z)$ = local jet radius (m)
t = time (s)
v = velocity
x_i = structural parameter for Maxwell element i (dimensionless)

Greek Letters

δ = convective derivative, Eq. 9
ϵ = extensional strain (dimensionless)
$\dot{\epsilon}$ = extensional strain rate (s^{-1})
$\dot{\gamma}$ = magnitude of shear rate (s^{-1})
$\overline{\dot{\gamma}}$ = average of $\dot{\gamma}$ over a cross section (s^{-1})
$\underline{\underline{\dot{\gamma}}}$ = shear rate tensor
η = shear viscosity (Pa·s)
ρ = density (kg/m^3)
σ_s = surface tension (N/m)
$\underline{\underline{\sigma}}$ = stress tensor
$\underline{\underline{\sigma_i}}$ = contribution to the stress tensor from Maxwell element i
τ_i = relaxation time of Maxwell element i (s)
φ = cone angle of the nozzle (dimensionless)

LITERATURE CITED

Acierno, D., F. P. La Mantia, G. Marrucci, and G. Titomanlio, "A nonlinear viscoelastic model with structure-dependent relaxation times: I. Basic formulation," *J. Non-Newtonian Fluid Mech.*, **1**, 125 (1976).

Agrawal, P. K., W. K. Lee, J. M. Lorntson, C. I. Richardson, K. F. Wissbrun, and A. B. Metzner, "Rheological behavior of molten polymers in shearing and in extensional flows," *Trans. Soc. Rheol.*, **21**, 355 (1977).

Bankar, V. G., J. E. Spruiell, and J. L. White, "Melt spinning dynamics and rheological properties of Nylon 6," *J. Appl. Polym. Sci.*, **21**, 2135 (1977).

Cable, P. J., and D. V. Boger, "A comprehensive experimental investigation of tubular entry flow of viscoelastic fluids," *AIChEJ.*, **24**, 869 (1978).

Chang, J. C., and M. M. Denn, "An experimental study of isothermal spinning of a Newtonian and a viscoelastic liquid," *J. Non-Newtonian Fluid Mech.*, **5**, 369 (1979).

Cogswell, F. N., "Converging flow and stretching flow: a compilation," *J. Non-Newtonian Fluid Mech.*, **4**, 23 (1978).

De Cleyn, G., "Elastische effecten by de stroming van polymeren," Ph.D. dissertation, Katholieke Universiteit Leuven (1980).

De Cleyn, G., and J. Mewis, "A constitutive equation for polymer liquids: application to shear flow," *J. Non-Newtonian Fluid Mech.*, **9**, 91 (1981).

Denn, M. M., "Extensional flows: experiment and theory," *The mechanics of viscoelastic fluids*, R. S. Rivlin, ed., p. 101, ASME, New York (1977).

Denn, M. M., "Continuous drawing of liquids to form fibers," *Ann. Rev. Fluid Mech.*, **12**, 365 (1980).

Fisher, R. J., M. M. Denn and R. I. Tanner, "Initiale profile development in melt spinning," *Ind. Eng. Chem. Fund.*, **19**, 195 (1980).

Kanel, F. A., "The extension of viscoelastic materials," Ph.D. Thesis, Univ. of Delaware (1972).

Lodge, A. S., *Body tensor fields in continuum mechanics (with applications to polymer rheology)*, Academic Press, New York (1974).

Mewis J., "Thixotropy—a general review," *J. Non-Newtonian Fluid Mech.*, **6**, 1 (1979).

Middleman, S., *Fundamentals of Polymer Processing*, McGraw-Hill, New York (1977).

Oliver, D. R., and R. C. Ashton, "The triple jet: influence of shear history on the stretching of polymer solutions," *J. Non-Newtonian Fluid Mech.*,

1, 93 (1976).
Petrie, C. J. S., *Elongational Flows*, Pitman, London (1979).
Phan-Thien, N., "A nonlinear network viscoelastic model," *J. Rheol.*, **22**, 259 (1978).
Spearot, T. A., and Metzner, A. B., "Isothermal spinning of molten polyethylenes," *Trans. Soc. Rheol.*, **16**, 495 (1972).
Ziabicki, A., *Fundamentals of Fibre formation*, J. Wiley, New York (1976).

Manuscript received June 29, 1981; revision received January 25, and accepted February 22, 1982.

Bed-Surface Contact Dynamics for Horizontal Tubes in Fluidized Beds

The local contact characteristics between the bed emulsion and the tube surface for horizontal tubes immersed in fluidized beds were investigated experimentally. The measurements indicated that the contact dynamics change significantly with circumferential position, gas flow rate, particle size and system pressure. From the experimental data, quantitative information on the local fluidization behavior were generated for use in heat transfer models.

RAVI CHANDRAN and J. C. CHEN

Institute of Thermo-Fluid Engineering & Science
Lehigh University
Bethlehem, PA 18015

SCOPE

Many applications of fluidized beds involve heat transfer to or from submerged tubes and tube bundles. Measurements of heat transfer between fluidized beds and horizontal tubes have been carried out by many investigators and both experimental data and correlations are reported in the literature (Saxena et al., 1978). However, as pointed out by Chandran et al. (1980), the conventional approach of relating heat transfer coefficients and operating parameters by means of empirical correlations seems to be inadequate.

A number of researchers have attempted the mechanistic approach and have developed semi-empirical relations for the heat transfer coefficient (Chandran, 1980). In order to examine the validity of the models that have been proposed, it is necessary to know the transient contact characteristics between the bed emulsion and the tube surface on a local basis. Until recently, a lack of such knowledge hampered the development and use of phenomenological models (Chen, 1976; Rooney and Harrison, 1976; Ozkaynak and Chen, 1980). From a design standpoint, there is a need for improved phenomenological understanding of the mechanisms and appropriate modeling of the transport processes. The objectives of this work were to generate the necessary information and to facilitate the development of a mechanistic model for the heat transfer process.

The experiments were performed in two different fluidized bed test facilities. Measurements were obtained in air-fluidized beds of glass beads for both a single tube and a ten-row bare tube bendle configuration. The capacitance probe technique, developed by Ozkaynak and Chen (1978) for contact measurements on a vertical tube, was used to investigate the dynamic characteristics of local fluidization behavior around horizontal tubes. Data were obtained for four different particle sizes (dia. ranging from 245 to 1580 μm), at three different system pressures (101.3, 202.6 and 405.3 kPa) and over a range of air flow rates (up to 12 times the minimum fluidization flow rate). The capacitance measurements were made at angular positions 90° apart around the circumference of the test tube in the case of single tube experiments and at 45° intervals in the case of multi-tube experiments.

CONCLUSIONS AND SIGNIFICANCE

The capacitance signals indicated distinctly different bed-surface contact characteristics at various angular positions around the tube. At low gas flow rates, the top surface of the tube remained covered by an essentially quiescent cap of densely packed particles with very long contact times and with no apparent displacement by passing bubbles. At the sides of the tube, a renewal type of contact with distinct periodic variations in the emulsion density was found. A different behavior was observed at the bottom of the tube. This segment was seen to encounter a relatively light-density emulsion with little fluctuation in the instantaneous density. A variation in the gas flow rate resulted in a marked change in the transient contact behavior. With an increase in the gas flow rate, the top of the tube experienced increasingly more effective scrubbing by passing bubbles and the stagnant cap was replaced by distinct "packets" of particles. The sides of the tube encountered more and more of the dilute void-phase, while the bottom portion of the tube experienced a renewal type of contact with the dense-phase packet contribution becoming important.

Quantitative information on the local fluidization characteristics were obtained by differentiating between a "dense phase" and a "lean phase" contact at the tube surface. The capacitance signals were processed to determine the values of the following parameters—root-square-average residence time of the dense phase, fractional contact time of the lean phase, and the average void fractions of the dense and the lean phases. The magnitude of these quantities were found to strongly depend upon circumferential position, gas flow rate, particle size and

Correspondence concerning this paper should be addressed to Ravi Chandran. He is now in the Department of Mechanical Engineering, Ohio University, Athens, OH 45701.
0001-1541-82-5353-0907-$2.00